

## Non-linear FE Analysis of RC Deep Beams with openings Strengthened with CFRP Composites

R. A. Hawileh<sup>1</sup>, T. A. El-Maaddawy<sup>2</sup>, and M. Z. Naser<sup>3</sup>

<sup>1</sup>American University of Sharjah, Sharjah, UAE

<sup>2</sup>United Arab Emirates University, Al-Ain, UAE

<sup>3</sup>American University of Sharjah, Sharjah, UAE

**ABSTRACT:** This study is aimed at developing a 3D nonlinear finite element (FE) model that can simulate the response of reinforced concrete (RC) deep beams with openings strengthened in shear with carbon fiber reinforced polymer (CFRP) sheets. The opening is located at the mid-point of the shear span so that it fully interrupts the natural load path. The FE model is developed and the simulation environment is conducted using the commercial finite element code, ANSYS. The concrete material is modeled using solid elements that account for concrete cracks and other material nonlinearities. Multilayer Shell elements are used to model the CFRP sheets along with their adhesive. Link elements are used to model the internal steel reinforcement. The FE model accounts for the bond behavior at the concrete-to-CFRP interface by introducing a layer of epoxy at the interface between the concrete and the CFRP. The results of the FE model are in good agreement with the experimental data.

### 1 INTRODUCTION

The use of externally bonded carbon fiber reinforced polymer (CFRP) composite sheets to strengthen reinforced concrete (RC) beams deficient in shear strength has gained wide acceptance in the construction engineering community. Numerous studies demonstrated the effectiveness of externally bonded CFRP composites to improve the shear capacity of shallow RC beams (Chaallal et al. 2002; Khalifa & Nanni 2002; Leung et al. 2007). The viability of CFRP to enhance the shear capacity of shallow RC beams containing openings has also been reported in the literature by few researchers (Abdalla et al. 2003; Pimanmas 2010). Few researchers investigated the behavior of RC deep beams strengthened with CFRP composites (Islam et al. 2004; Zhang et al. 2004). Very little information is available on the behavior of RC deep beams with openings strengthened with CFRP. Results of a recent study indicate that the application of CFRP composite sheets around the openings in deep beams is an effective solution to improve the shear capacity (El-Maaddawy & Sherif 2009).

The analysis of RC deep beams with openings is a complex problem. The application of CFRP composites around the openings as a structural engineering solution to improve the shear capacity makes the problem more complex. Current codes of practice provide little guidance in this regard, and hence an appropriate and consistent approach for performance prediction of such unusual structural concrete members is required.

This paper presents a 3D nonlinear finite element (FE) model, developed using the commercial finite element code, ANSYS, to simulate the response of tested RC deep beams with openings strengthened in shear with CFRP composites tested by El-Maaddawy & Sherif 2009. The results obtained from the FE analysis are compared with the experimental data of four RC deep beams with openings. The numerical results are presented in terms of the ultimate load carrying capacity, crack pattern, and deformational characteristics. The comparisons between the FE

results and the experimental data demonstrate the accuracy and validity of the FE model. The FE modeling of the problem can serve as a numerical platform for performance prediction of RC deep beams with openings strengthened in shear with CFRP composites.

## 2 FINITE ELEMENT MODEL DEVELOPMENT

The main objective of this study is to build a viable 3D non-linear FE model that is able to accurately predict the behavior of RC deep beams with openings strengthened with CFRP sheets. Four 3D nonlinear FE models are developed using the simulation environment, ANSYS 11.0 (2007). The developed FE models presented herein are based on the tested specimens in El-Maaddawy & Sherif 2009 experimental program; hence they have the same dimensions, geometry and material configurations, boundary conditions, and loading. Table 1 demonstrates the experimental and numerical matrix used in this study. The experimental specimen designation listed in Table 1 starts with the prefix "NS" or "FS" to represent if the specimen is non-strengthened or strengthened using CFRP sheets, respectively. The three numerical figures after the designation letters are used to refer to the opening size in (mm), followed with the letter "C" to specify that the location of the opening is located at the center of the shear span. In order to distinguish between the experimental specimens and numerical models, the prefix "FE" is added to the labeling of the FE models.

Table 1. Experimental and numerical matrix used

Specimen	FE Model	Opening location	Opening size (mm)	External FRP strengthening
NS-200-C	FE NS-200-C	Middle of shear span	200 × 200	No
NS-250-C	FE NS-250-C	Middle of shear span	250 × 250	No
FS-200-C	FE FS-200-C	Middle of shear span	200 × 200	Yes
FS-250-C	FE FS-250-C	Middle of shear span	250 × 250	Yes

### 2.1 Geometry

The tested specimen shown in Figure 1 is 1200 mm long with a rectangular cross section of 80 × 500 mm. The RC deep beam had a clear span of 1000 mm giving a span-to-depth ratio of 2. The tension steel reinforcement consisted of four No. 14 steel bars while the compression steel reinforcement consisted of two No. 8 steel bars. The web reinforcement consisted of No. 6 bars, spaced at 150 mm in both vertical and horizontal directions. A clear cover of 15 mm was maintained at the top and bottom of the beam whereas a clear cover of 10 mm was maintained on the beam's vertical sides. In order for the CFRP strengthening system to be effective, the CFRP sheets were attached both horizontally and vertically around the four sides of the opening to interrupt the potential shear cracks once they were loaded. Longitudinal CFRP sheets were first bonded to sides of the beams above and below the opening with their fibers oriented parallel to the longitudinal axis of the beam. Afterwards, CFRP sheets with fibers oriented in the vertical direction were wrapped above and below each opening. To mimic the presence of a RC slab a U-shaped CFRP sheet was wrapped around the top chord above the opening leaving a clear distance of 25 mm at the top of the beam while, the bottom chord below the opening was fully wrapped with a CFRP sheet having an overlap of about 60 mm. At the end, vertical CFRP sheets were then placed adjacent to each vertical face of the openings with fibers oriented in a direction parallel to the transverse axis of the beam to restrict the growth of any diagonal cracks that might originate at the openings' corners as well as providing more anchorage for the longitudinal CFRP sheets above and below the openings. A detailed description of the CFRP

strengthening scheme can be found in the experimental study conducted by El-Maaddawy & Sherif 2009.

Due to the symmetry of the geometry, loading, boundary conditions, and material properties, a quarter model was built and analyzed. Figure 2 shows an isometric view of the developed model with the boundary conditions and loading. As shown in Figure 2 that the developed model has two planes of symmetries in two principal axes. The advantage of building a quarter model for this structure is the reduction in the total number of elements (by four) which will result in saving a lot of computational time.

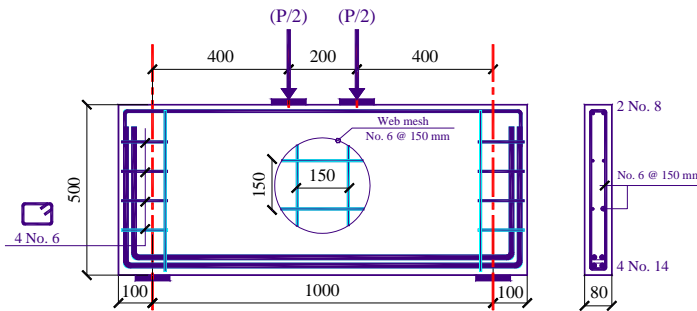


Figure 1. Specimen details and test set up (El-Maaddawy & Sherif 2009)

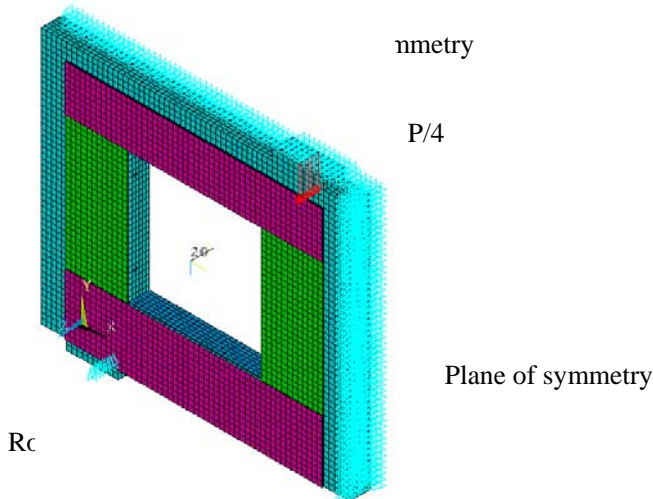


Figure 2. FE quarter model and boundary conditions

## 2.2 Element Types and Meshing

The concrete material was simulated using SOLID65 ANSYS (2007) elements. SOLID65 is capable of modeling the nonlinear behavior of concrete either by cracking in tension or crushing in compression. In addition, SOLID65 has 8 nodes; each node of the solid element has three translational degrees of freedom in the x, y, and z directions. The steel bars reinforcements were modeled using LINK8 ANSYS 2007 element. LINK8 is defined by two nodes with three translational degrees of freedom at each node. The element is capable of elastic-plastic deformation, stress stiffening, and large deflection. In addition, perfect bond between the concrete and reinforcement steel was assumed in this study through sharing the same nodes (De

Lorenzis & Teng 2007). The CFRP sheets are modeled using SHELL99 ANSYS 2007 element with elastic orthotropic material properties that have its own coordinate system, where the x-axis is in the direction parallel to the fibers. SHELL99 element is used to model layered applications of structural shell models. The element allows up to 250 layers and has eight nodes with six degrees of freedom at each node: translations in the x, y, and z directions and rotations about the x, y, and z-axes. In this study, the first layer of SHELL99 is used to simulate the epoxy resin at the concrete/CFRP sheet interface while the following layers are used to simulate the CFRP sheets, both horizontally and vertically depending on the location of the FRP element. The coordinate system for each layer of the SHELL99 elements is specified depending on the orientation of the CFRP fibers, horizontally or vertically.

### 2.3 Material Constitutive Models and Properties

The concrete nonlinear material behavior in compression is modeled using the relationship given in Eq. 1 (Park & Paulay 1975).

$$f_c = \begin{cases} f_c' \left[ \frac{2\varepsilon_c}{\varepsilon_{co}} - \left( \frac{\varepsilon_c}{\varepsilon_{co}} \right)^2 \right] & \text{for } 0 \leq \varepsilon_c \leq \varepsilon_{co} \\ f_c' - \frac{0.15 f_c'}{(\varepsilon_{cu} - \varepsilon_{co})} (\varepsilon_c - \varepsilon_{co}) & \text{for } \varepsilon_{co} \leq \varepsilon_c \leq \varepsilon_{cu} \end{cases} \quad (1)$$

where  $f_c$  = concrete compression stress,  $f_c'$  = concrete compression strength,  $\varepsilon_c$  = concrete strain, and  $\varepsilon_{co}$  = concrete strain corresponding to  $f_c'$ , and  $\varepsilon_{cu}$  = ultimate concrete strain (0.0038). The ultimate compressive strength was 21MPa along with a Poisson's ratio of 0.2. The concrete tensile stress-strain response is modeled using a linear elastic behavior up to the tensile rupture strength ( $f_r$ ). The tensile rupture strength is taken as  $0.62\sqrt{f_c'}$ . After reaching the peak tensile stress, a tensile stress relaxation is simulated by a sudden drop in the concrete tensile strength to  $0.6f_t$ . Afterwards, the tensile stress-strain curve descends linearly to zero stress at a strain of  $6\varepsilon_t$ , where  $\varepsilon_t$  = concrete strain corresponding to  $f_r$ . In addition, the Von-Mises failure criterion for the steel reinforcement is used to define failure of the reinforced concrete.

The main longitudinal steel reinforcement was Grade 420 while the web vertical reinforcement was Grade 300. The longitudinal and vertical steel reinforcement had a modulus of elasticity of 200GPa and a Poisson's ratio of 0.3 but with different yield strength of 420MPa and 300MPa, respectively. The nonlinear material property of steel was assumed to be elastic-perfectly plastic. The epoxy resin (Sikadur 330) used to bond the carbon fiber fabric (SikaWrap Hex 230C ) to the concrete surface had a tensile strength of 30MPa and an ultimate elongation of 1.5%. An assumed layer of epoxy having a thickness of 1mm was used to simulate a bond layer at the CFRP to concrete interface. According to the data sheet of the manufacturer (Sika2005), a cured CFRP composite sheet (SikaWrap Hex 230C carbon fiber fabric cured with Sikadur 330 epoxy resin) has a typical thickness of 0.381mm, an average tensile strength of 894MPa, a tensile elastic modulus of 65.4GPa, and an ultimate elongation of 1.33%. The cured CFRP composite sheet (SikaWrap Hex 230C carbon fiber cured with Sikadur 330 epoxy resin) was treated as an elastic orthotropic material up to failure to simulate its natural behavior. The elastic orthotropic material properties used are [ $E_x = 65\text{GPa}$ ,  $E_{y,z} = 5.87\text{GPa}$ ,  $\nu_{xy,yz} = 0.28$ ,  $\nu_{yz} = 0.42$ ,  $G_{xy,xz} = 2.9\text{GPa}$ , and  $G_{yz} = 2.2\text{GPa}$ ]. The monotonic loading and vertical restrains were applied on two rigid supports presenting a loading support and a roller. This is simulated using SOLID45 ANSYS (2007) elements with rigid elastic steel's material properties. Such technique would prevent any major stress concentration on the concrete material at those locations.

## 2.4 Failure Criteria

For the strengthened RC deep beams, The FE models are assumed to fail by debonding if the strain at the of the CFRP sheets exceeds the smaller of  $0.75\varepsilon_{fu}$  or 0.004 (ACI 440 2008) where  $\varepsilon_{fu}$  is the design rupture strain of the CFRP reinforcement (ACI 440, 2008). According to the manufacturer  $\varepsilon_{fu}$  is 1.09% which leads to  $0.75\varepsilon_{fu}$  of 0.0082.

## 3 RESULTS AND DISCUSSION

The validation of the FE models was conducted by comparing the load-deflection response of the experimental and FE models for the four specimens simulated, herein. A comparison between the experimental and predicted load-deflection response is presented in Figure 3. A comparison between the predicted load capacity, the deflection at failure and the associated results obtained from experimental testing is shown in Table 2.

Table 2. Model Validation

Specimen	FE Model	Failure Load (KN)		Percentage Difference 1-(Exp./FE)	Maximum Deflection (mm)		Percentage Difference 1-(Exp./FE)
		Exp.	FE		Exp.	FE	
NS-200-C	FE NS-200-C	163.0	160	1.80%	4.1	4.15	-1.2%
NS-250-C	FE NS-250-C	110.08	106.6	3.3%	5.7	6.1	-6.6%
FS-200-C	FE FS-200-C	270.5	270	0.2%	5.2	5.7	-8.8%
FS-250-C	FE FS-250-C	182.0	186	-2.2%	5.4	5.1	5.6%

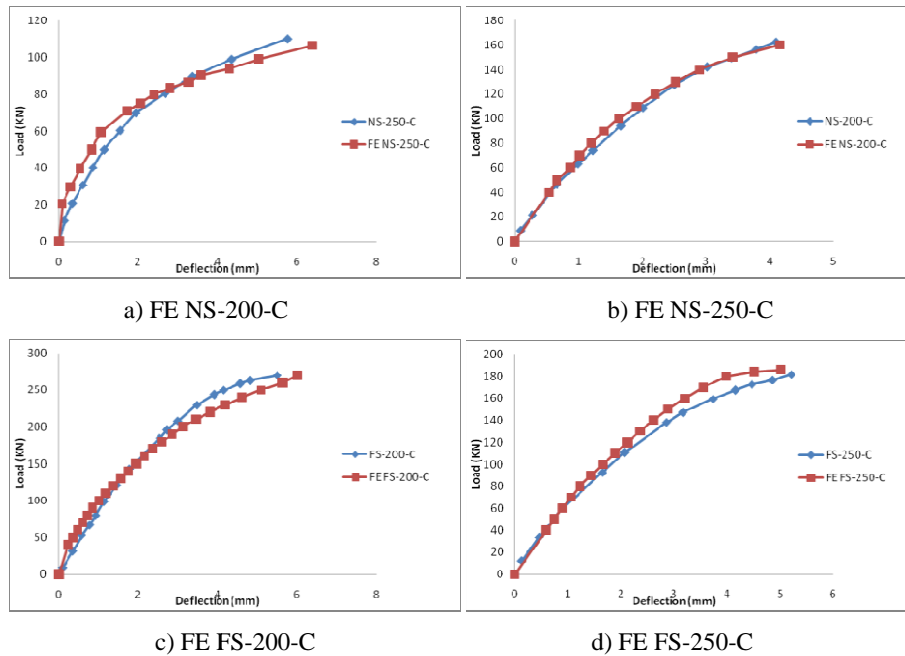


Figure 3. Comparison between the experimental and FE models

It is clear from Figure 3 that there is a good matching between the experimental and FE load-deflection response at all stages of loading till failure. This indicates the validity of the proposed FE models and reliability of FE simulation. Furthermore, Table 2 draws a detailed comparison between the predicted failure load and mid-span deflection. Upon comparison of the failure load, it is evident that FE models predicted the failure load with less than 3.5% range difference. In the “FE FS-250-C” case, the FE simulation seems to overestimate the failure load by 2.2%, while it underestimates the failure load for the other cases by 1.8, 3.3 and 0.2% differences for the “FE NS-200-C”, “FE NS-250-C” and “FE FS-200-C” models, respectively. In the same manner, the case of “FE FS-250-C” underestimated the maximum deflection at failure by 5.6% while the rest of the FE models overestimated the maximum deflection at failure by 1.2%, 6.2% and 8.8% for the “FE NS-200-C”, “FE NS-250-C” and “FE FS-200-C” models, respectively.

It is clear that whenever the size of the opening decreases, the capacity of the RC deep beam increases. In the same manner, the performance of the strengthened beams achieved higher ultimate loads than those without external CFRP sheets strengthening systems. For instance, about 69% and 75% increases in the capacity were noticed on the “FE FS-200-C” and FE FS-250-C cases over their unstrengthened counterparts, FE NS-200-C and FE NS-250-C, respectively. In addition to the effect of external strengthening, the increase of size of the opening from  $200 \times 200\text{mm}$  to  $250 \times 250\text{mm}$  reduced the capacity of the RC deep beams. The capacity of the unstrengthened model FE NS-250-C case was dropped by about 33% over the same model with smaller size opening FE NS-200-C. Similarly, the capacity of the model specimen FE FS-250-C was lower than that of the FE FS-200-C model by about 31%. It is evident that the size of the opening as well as the availability of the strengthening scheme has a significant influence on the behavior of RC deep beams.

Figure 4 shows that the crack pattern observed experimentally in specimen NS-250-C and predicted by the model FE NS-250-C at failure. The principal compressive stresses at ultimate in the model FE NS-250-C is also shown in the same figure (Figure 4c). It is clear that there is a good matching between the observed and predicted crack patterns which prove the capability of the FE model to accurately predict the crack pattern. It is evident that the location and direction of the principal compressive stresses are consistent with the crack pattern. It can also be seen that the compressive stresses are a maximum at the bottom right corner of the opening which indicates that concrete failure initiated at this location. Similar behavior was also observed experimentally as shown in Figure 4a.

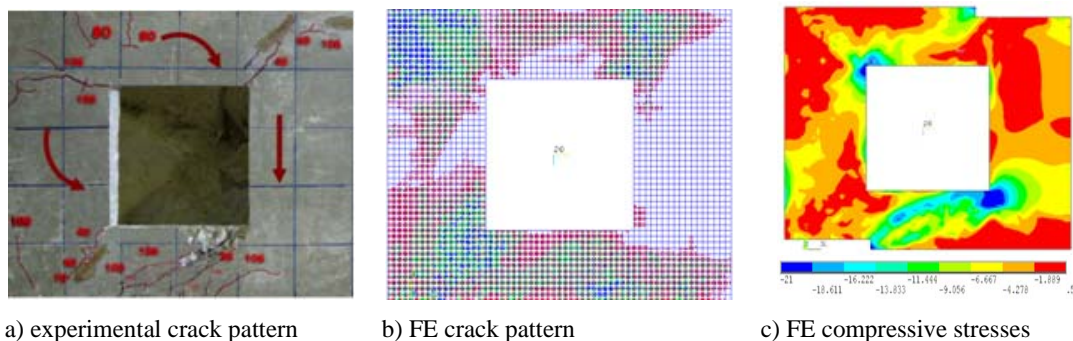


Figure 4. Crack patterns and principal compressive stresses in MPa of the specimen NS-250-C

#### 4 SUMMARY AND CONCLUSION

Four nonlinear finite element models were developed in this study to simulate the response RC deep beams with openings non-strengthened and strengthened using externally bonded CFRP sheets. The FE models are validated by comparing the FE results with the results of the experimental tests conducted by El-Maaddawy & Sherif 2009. Overall comparison between the ultimate load, mid-span deflection, and crack patterns showed good agreement between the results of the experimental tests and the FE simulation models. Based on the results of this study, the following conclusion can be drawn:

- The load-deflection response of the FE models is in a good agreement with the measured experimental response.
- The FE simulation models confirmed that the size of the opening and the presence of the CFRP strengthening have a significant influence on the performance of RC deep beams. The larger the opening size, the more likely the RC deep beam to fail prematurely. The CFRP strengthening around the openings resulted in up to a 75% increased the shear capacity.
- The developed FE models verified in this study could be used as an alternative to experimental testing, which is usually more costly and time extensive. The FE modeling of the problem can also serve as a numerical platform for performance prediction of RC deep beams with openings strengthened in shear with CFRP composites.

#### 5 REFERENCES

- Abdalla, HA, Torkey, AM, Haggag, HA, and Abu-Amira, AF. 2003. Design against cracking at openings in reinforced concrete beams strengthened with composite sheets. *Composite Structures*, 60:197–204
- ANSYS – Release Version 11. A Finite Element Computer Software and User Manual for Nonlinear Structural Analysis, ANSYS 2007; Inc. Canonsburg, PA.
- Chaallal, O, Shahawy, M, and Hassan, M. 2002. Performance of reinforced concrete T-girders strengthened in shear with carbon fiber-reinforced polymer fabric. *ACI Structural Journal*, 99: 335–43.
- De Lorenzis, L and Teng, JG. 2007. Near-surface mounted FRP reinforcement: an emerging technique for strengthening structures. *J Compos, Part B*; 38:119–43.
- El-Maaddawy, T and Sherif, S. 2009. FRP composites for shear strengthening of reinforced concrete deep beams with openings. *Composite Structures*, 89: 60-69.
- Islam, M, Mansur, M, and Maalej, M. 2004. Shear strengthening of RC deep beams using externally bonded FRP systems. *Cement and Concrete Composites*, 27:413–20.
- Khalifa, A and Nanni, A. 2002. Rehabilitation of rectangular simply supported RC beams with shear deficiencies using CFRP composites. *Construction and Building Materials*, 16: 135-146.
- Leung, CK, Chen, Z, Lee, S, Ng, M, Xu, M, and Tang, J. 2007. Effect of size on the failure of geometrically similar concrete beams strengthened in shear with FRP strips. *ASCE Journal of Composite Construction*, 11: 487-496.
- Park, R., and Paulay, T., *Reinforced Concrete Structures*, John Wiley and Sons, New York, 1975, 800 pp.
- Pimannas, A. 2010. Strengthening R/C beams with opening by externally installed FRP rods: Behavior and analysis. *Composite Structures*, 92: 1957-1976.
- Sika. SikaWrap Hex 230C: Carbon Fiber Fabric for Structural Strengthening System Product Data Sheet, Edition 04.2005, 2005.
- Zhang Z, Hsu, C, and Moren, J. 2004. Shear strengthening of reinforced concrete deep beams using carbon fiber reinforced polymer laminates. *ASCE Journal of Composite Construction*, 8:403–14.